Highlight Review

Applications of Single-site Photocatalysts Implanted within the Silica Matrixes of Zeolite and Mesoporous Silica

Hiromi Yamashita* and Kohsuke Mori

(Received November 6, 2006; CL-068013)

Abstract

The tetrahedrally coordinated metal oxide (titanium, vanadium, chromium, and molybdenum oxides) moieties can be implanted and isolated in the silica matrixes of microporous zeolite and mesoporous silica materials and named as "single-site photocatalysts." Under UV-light irradiation these single-site photocatalysts form the charge-transfer excited state, i.e., the excited electron–hole pair state which localizes quite near to each other as compared to the electron and hole produced in semiconducting materials, plays a significant role in various photocatalytic reactions. Especially, the single-site titanium oxide photocatalyst demonstrates the high reactivity and selectivity under UV-light irradiation, while the single-site chromium oxide operates as a visible-light sensitive photocatalyst. These single-site photocatalysts not only can promote photocatalytic reactions but also can be utilized to synthesis of functional materials. The transparent mesoporous thin film with single-site photocatalyst generates the superhydrophilic surface. The nano-sized metal catalyst can be photodeposited on the excited single-site photocatalyst under UV-light irradiation.

♦ Introduction

The tetrahedrally coordinated metal oxide (titanium, vanadium, chromium, and molybdenum oxides (Ti, V, Cr, and Mo oxides)) moieties can be implanted and isolated in the silica matrixes of microporous zeolite and mesoporous silica materials[1–20] and named as "single-site photocatalysts." The single-site catalysts can be implanted in silica matrixes (Si/Me $>$ 30; Me $=$ Ti, V, Cr, etc.) by various anchoring techniques (hydrothermal synthesis, sol–gel method, chemical vapor deposition, etc.) and stable as far as the silica matrixes keep their porous structures. Under UV-light irradiation these single-site photocatalysts form the charge-transfer excited state, i.e., the excited electron–hole pair state which localizes quite near to each other as compared to the electron and hole produced in semiconducting materials, plays a significant role in various photocatalytic reactions. Especially, the single-site Ti oxide photocatalyst demonstrates the high reactivity and selectivity under UV-light irradiation, while the single-site Cr oxide operates as a visible-light sensitive photocatalyst. These single-site photocatalysts not only can promote photocatalytic reactions but also can be utilized to synthesis of functional materials. The transparent mesoporous thin film with single-site photocatalyst generates the superhydrophilic surface. The nano-sized metal catalyst can be photodeposited on the excited single-site photocatalyst under UV-light irradiation (Figure 1).

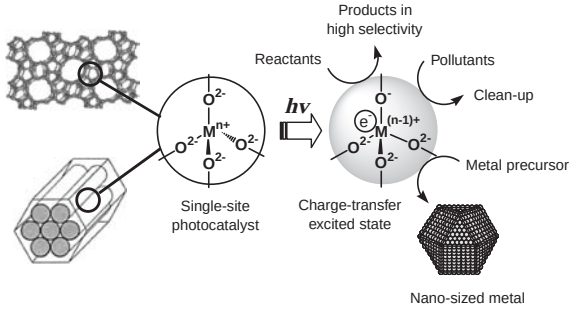

Figure 1. The formation of charge-transfer excited state with tetrahedrally coordinated metal oxide moieties under UV-light irradiation and their applications to the photocatalytic reactions and the synthesize of nanosized metal catalyst.

♦ Unique Reactivity on Single-site Photocatalyst

The Ti oxide moieties included within the framework of zeolite materials have been revealed to have a unique local structure as well as a high selectivity in the oxidation of organics with hydrogen peroxide.[1–4] The Ti-containing zeolites (TS-1 and Ti-β) and mesoporous silica (Ti-MCM and Ti-HMS) have been synthesized[5–9,12–26] and can be utilized as the efficient single-site photocatalysts. In situ photoluminescence, ESR, UV–vis, and XAFS investigations indicated that the Ti oxide moieties implanted in zeolite materials exist as isolated moieties in a tetrahedral coordination. The photocatalytic reduction of CO_2 with H_2O is of interest as a reaction system utilizing artificial photosynthesis.[5–9,17–20] It was found that the single-site Ti oxide photocatalyst in zeolite materials exhibits a high and unique reactivity as compared to bulk TiO_2 powder.[5–9,17–20] UV-irradiation of the TS-1 zeolite and the Ti-containing mesoporous silica

*Prof. H. Yamashita**
Division of Materials and Manufacturing Science, Graduate School of Engineering, Osaka University, 2-1 Yamada-oka, Suita, Osaka 565-0871
Research Center for Solar Energy Chemistry, Osaka University, Toyonaka, Osaka 560-8531
E-mail: yamashita@mat.eng.osaka-u.ac.jp
Dr. K. Mori
Division of Materials and Manufacturing Science, Graduate School of Engineering, Osaka University, 2-1 Yamada-oka, Suita, Osaka 565-0871
E-mail: mori@mat.eng.osaka-u.ac.jp

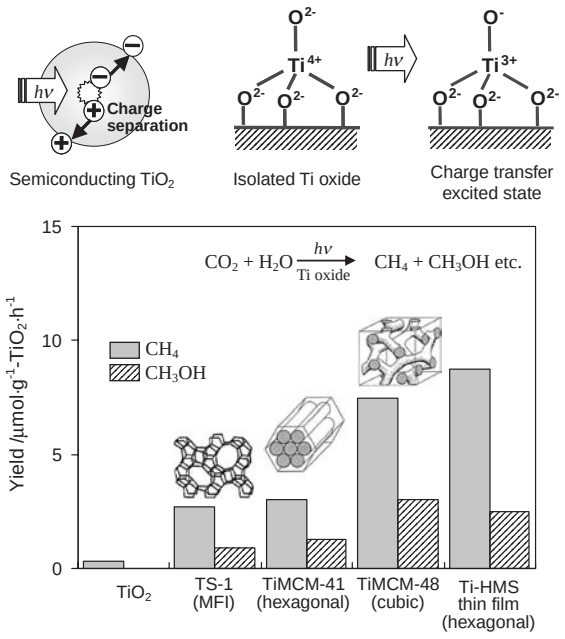

Figure 2. The product distribution of the photocatalytic reduction of CO_2 with H_2O on various Ti oxide photocatalysts.

in the presence of CO_2 and H_2O led to the formation of CH_3OH and CH_4 as the main products.[17–20] As shown in Figure 2, Ti-MCM-48 (pore size $>$ 2 nm, 3-D channel) exhibits much higher reactivity than TS-1 (ca. 0.6 nm, 3-D), Ti-MCM-41 (pore size $>$ 2 nm, 1-D), and powdered TiO_2. The higher reactivity and higher selectivity for the formation of CH_3OH observed with the Ti-MCM-48 may be due to the combined contribution of the high dispersion state of the Ti oxide moieties and the large pore size with a 3-D channel structure. These results strongly indicate that mesoporous silica with single-site Ti oxide photocatalyst is promising candidates as effective photocatalysts and also indicates that the charge-transfer excited state of Ti oxide moieties plays an important role in photocatalytic reduction of CO_2 with H_2O to produce CH_3OH. The unique selectivity on the single-site Ti oxide photocatalyst implanted in zeolite materials can also be observed in various reactions such as NO decomposition and oxidation of hydrocarbon. For example, UV-light irradiation of the powdered TiO_2 and the Ti oxide highly dispersed on zeolite cavity and framework in the presence of NO were found to lead to the evolution of N_2, O_2, and N_2O with different selectivities.[12–16] The tetrahedrally coordinated single-site Ti oxide moieties implanted in zeolite materials exhibited a high reactivity and a high selectivity for the formation of N_2 while the formation of N_2O was found to be the major reaction on the bulk TiO_2 as well as on the catalysts with aggregated octahedrally coordinated Ti oxide. These results indicate that the single-site Ti oxide photocatalyst in zeolite materials can have high catalytic efficiency and selectivity.

♦ *Single-site Photocatalyst with Controlled Hydrophobic–Hydrophilic Surface*

The H_2O affinity of Ti-containing zeolites changes significantly depending on the preparation methods, and their hydrophobic–hydrophilic properties can modify the photocatalytic properties.[19,20,24–26] Using the F^- media the hydrophobic zeolite and mesoporous silica can be synthesized. The interaction of Ti oxide moieties with H_2O molecules has been investigated by in situ XAFS measurement, because the change in the coordination geometry of Ti atom reflects very sensitively on the intensity and position of preedge peak in Ti K-edge XANES region.[1,8] As shown in Figure 3, the addition of H_2O molecules onto the Ti-β zeolites leads to the efficient decrease in the intensity of preedge peak and the shift to the higher energy in the peak position, indicating that the coordination number of Ti oxide moieties increases from its original four-coordination to five-coordination and finally to six-coordination. The changes in the peak intensity and position with the H_2O addition are more remarkable on the Ti-β (OH) prepared in OH^- media than Ti-β (F) prepared in the F^- media. The interaction between the added H_2O molecules and Ti oxide moieties in the zeolite framework is the higher in the pore of hydrophilic Ti-β (OH) than the hydrophobic Ti-β (F). The hydrophobic–hydrophilic properties of zeolite affect on the accessibility and the interaction between photocatalytic active sites (tetrahedrally coordinated Ti oxide moieties) and H_2O molecules and finally become the important factor to determine the photocatalytic reactivity and the selectivity. For

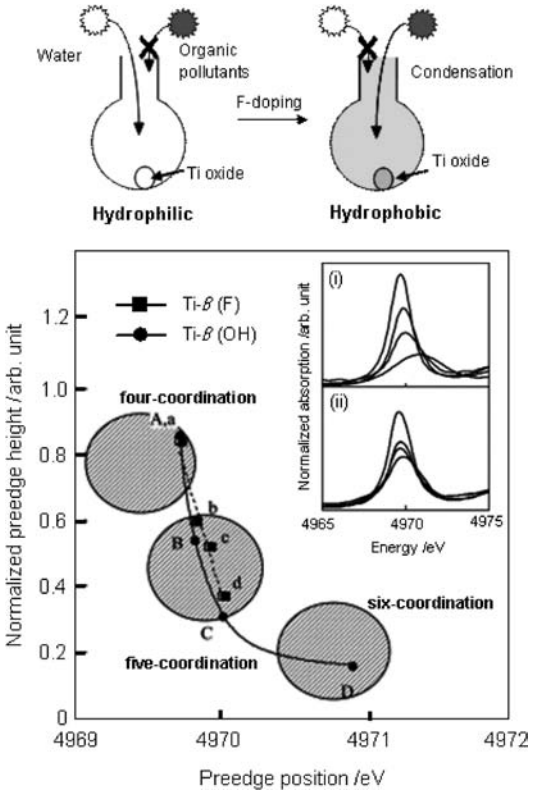

Figure 3. Plots of normalized height vs energy of the Ti preedge feature showing the values observed with Ti-β (OH) (A–D) and Ti-β (F) (a–d) zeolites in the absence and presence of added H_2O. The amount of the added H_2O; (A, a) 0, (B, b) 1.4, (C, c) 3.0, (D, d) 4.6 mmol/g·cat. The inset shows the effect of the addition of H_2O on the intensity and position of the preedge peak observed in the Ti K-edge XANES spectra of Ti-β (OH) (i) and Ti-β (F) (ii) zeolites. The amount of the added H_2O; 0, 1.4, 3.0, 4.6 mmol/g·cat (from top to bottom).

Published on the web (Advance View) February 3, 2007; doi:10.1246/cl.2007.348

example, in the photocatalytic reduction of CO_2 with H_2O to produce CH_4 and CH_3OH, the higher reactivity for the formation of CH_4 was observed with hydrophilic Ti-β (OH) and the higher selectivity for the formation of CH_3OH was observed with the hydrophobic Ti-β (F).[19,20] Furthermore, these hydrophobic zeolite materials exhibit the high ability for the adsorption of organic compounds diluted in water. The hydrophobic Ti-β (F) exhibited higher efficiency than the hydrophilic Ti-β (OH) for the photocatalytic degradation of organics (alcohols and organic halides) diluted water. The Ti oxide in the hydrophobic mesoporous silica HMS (F) doped with F^- ions also exhibited the efficient photocatalytic degradation.[24–26] The efficient photocatalytic degradation of organics diluted in water on these catalysts can be attributed to the larger affinity for the adsorption of organics on the Ti oxide moieties depending on the hydrophobic surface properties of the F^- ion-doped zeolite materials.

♦ *Visible-light Sensitive Single-site Photocatalyst*

The single-site Mo or Cr oxide photocatalyst can exhibit high activities for various reactions such as the photooxidation of hydrocarbons or the photoinduced metathesis of alkanes.[8] Especially, the single-site Cr oxide moieties implanted in mesoporous silica (Cr-HMS) show photocatalytic activities under not only UV-light but also visible-light irradiation.[27–38] As shown in Figure 4, Cr-HMS catalysts exhibit photoluminescence at around 550–750 nm upon excitation at around 520 nm. These absorption and photoluminescence can be attributed to the charge-transfer processes on the tetrahedrally coordinated Cr oxide moieties. These results indicate that the Cr-HMS involves Cr oxide moieties in tetrahedral coordination having terminal Cr=O, being in good agreement with the results obtained by the XAFS and UV–vis measurements. In the photoluminescence of the Cr-HMS, the fine structures can be observed which due to the vibration mode of Cr=O bonding. The energy separation between the bands for the vibronic transition in the Cr=O bond is more clear with Cr-HMS, while on the CrS-1 this band separation is very vague (Figure 4). The open space of mesopore of HMS is suitable to keep the isolated tetrahedrally coordinated Cr oxide moieties without the perturbation due to the neighboring surface OH groups.[27–31] The Cr-HMS showed photocatalytic reactivity for NO decomposition to produce N_2, N_2O, and O_2

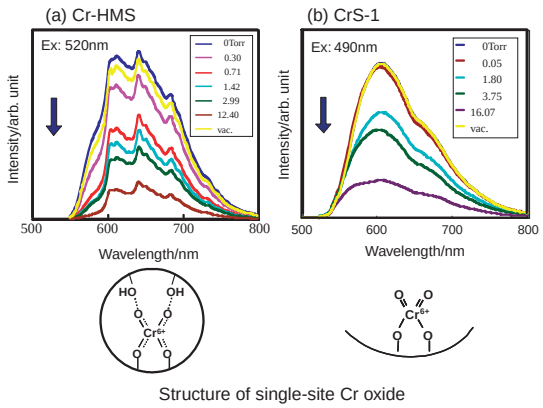

Figure 4. Photoluminescence spectra of Cr-HMS (a) and CrS-1 (b) and quenching by added propane.

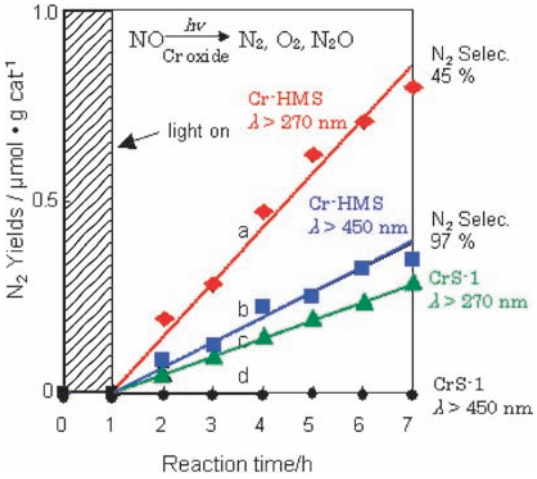

Figure 5. Reaction time profiles of the photocatalytic NO decomposition on Cr-HMS (a), (b) and CrS-1 (c), (d) under UV-light irradiation ($\lambda > 270$ nm) and visible-light irradiation ($\lambda > 450$ nm).

even under visible-light irradiation ($\lambda > 450$ nm), while no reaction was observed on the microporous CrS-1 zeolite (Figure 5). Visible-light irradiation ($\lambda > 450$ nm) of the Cr-HMS in the presence of propane and O_2 also led to the photocatalytic oxidation of propane to produce acetone, acrolein, CO_2/CO, etc. The partial oxidation of propane with a high selectivity for the production of oxygen-containing hydrocarbons proceeds under visible-light irradiation ($\lambda > 450$ nm), while further oxidation proceeds mainly under UV-light irradiation ($\lambda > 270$ nm) to produce CO_2. In these photocatalytic reactions, the selectivities under UV-light irradiation and visible-light irradiation were different. The tetrahedrally coordinated isolated Cr oxide moieties in HMS can exhibit the efficient photocatalytic reactivity even under visible-light irradiation with a high selectivity.

Recently, it was found that the binary metal oxide moieties, such as Cr, Ti oxides and V, Ti oxides, can be implanted in mesoporous silica using the photoassisted deposition and metal ion-implantation methods and these binary photocatalysts can demonstrate the high selectivity in the epoxidation of alkenes and alkanes under visible-light irradiation.[39,40]

♦ *Transparent Mesoporous Silica Thin Film with Single-site Photocatalyst*

The zeolite materials mentioned above are generally obtained in the form of powder. On the other hand, the thin film is an ideal morphology because of the combined properties of a tailored pore system and the inherent features of thin films. TiO_2 thin film is proven to exhibit superhydrophilic property under UV-light irradiation and applied as self-cleaning and antifogging materials.[41] It is of great importance to add the advantages of mesoporous structure and single-site photocatalyst to the thin film. The single-site photocatalyst (Ti and Cr) containing mesoporous silica thin films are strongly desired as the promising photoinduced functionalized materials.[42–44] The Ti-containing mesoporous silica (TMS) thin film (Ti/Si < 0.1) embedded onto the quarts plate can be prepared by the spin-coating sol–gel method. The synthesized mesoporous silica (MS) thin film with-

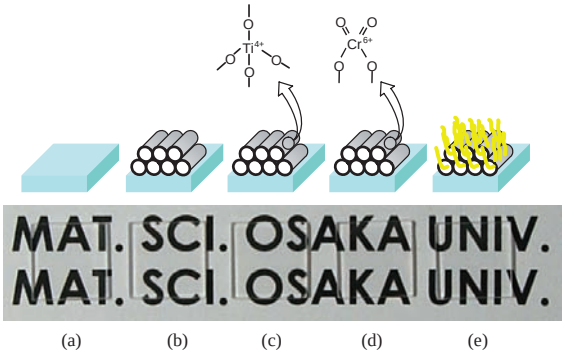

Figure 6. Sample photography of transparent thin films. (a) Quartz plate, and plates coated with (b) MS thin film, (c) TMS thin film (Ti/Si = 0.05), (d) CMS thin film (Cr/Si = 0.05), and (e) CMS thin film (Cr/Si = 0.05) after polymerization.

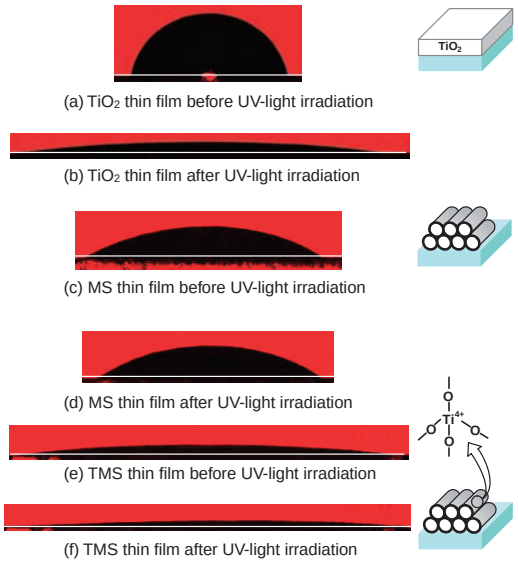

Figure 7. The images of water droplets observed before (a), (c), (e) and after (b), (d), (f) UV-light irradiation on TiO_2, mesoporous silica (MS), and Ti-containing mesoporous silica (TMS) thin films.

out Ti atoms and TMS thin film are colorless and completely transparent and well fixed on the substrate of quartz plate (Figure 6).[42–44] These samples exhibit a XRD diffraction peak at around 2–3° indicating the presence of hexagonally packed mesoporous structure. The results of XAFS and UV–vis absorption measurements indicate that the tetrahedrally coordinated Ti oxide moieties exist in the TMS thin film. The contact angle of the water droplet on these thin films was measured before and after UV-light irradiation (Figure 7). The water contact angle on TMS thin film before UV-light irradiation was 8°, which was much smaller than 72° on TiO_2 thin film and 22° on MS thin film. The presence of mesoporous structures of the TMS and MS thin films are found to responsible for the hydrophilic surface properties even before UV-light irradiation. The mesoporous structure can enhance the hydrophilicity owing to the capillary phenomenon, high surface polarity and large number of surface –OH group. Upon UV-light irradiation, the water contact angles on TMS thin film and TiO_2 thin film become extremely small

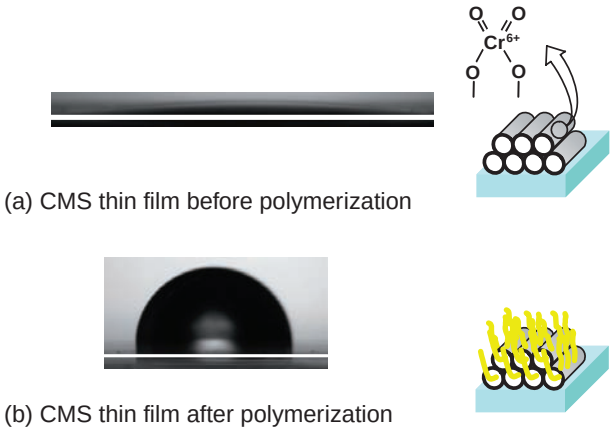

Figure 8. The images of water droplets on Cr-containing mesoporous silica (CMS) thin films (a) before and (b) after polymerization.

to perform the superhydrophilic property. The charge-transfer excited state of the tetrahedrally coordinated Ti oxide moieties formed under UV-light irradiation plays a significant role in the photoinduced superhydrophilic property. The transparent Cr-containing mesoporous silica (CMS) thin film can be also synthesized by sol–gel/spin-coating method.[43,44] The results of the XRD, XAFS, and UV–vis absorption measurements indicated the formation of tetrahedrally coordinated Cr oxide moieties in the CMS thin film. Interestingly, the CMS thin film with tetrahedrally coordinated Cr oxide moiety showed superhydrophilic properties even under visible-light irradiation.[43–46] Based on the polymerization ability of single-site Cr oxide moieties, the polyethylene can be synthesized on CMS surface with the aim of modification of the surface from hydrophilic into hydrophobic. As expected, the water contact angle of the sample after polymerization greatly increases up to 103°, which is much larger than that on untreated one (Figure 8) indicating that the surface of the CMS can be converted to be hydrophobic.

♦ *Synthesis of Nano-sized Metal Using Single-site Photocatalyst*

Nano-sized metal catalysts such as Pd, Pt, Ag, and Au have attracted a great deal of attention for their unique catalytic functions.[47–49] The development of convenient method to prepare nano-sized metals loaded on supports with controlled particle size is essential to design of the highly active metal catalysts. The metal precursor species can be easily deposited on the excited state of single-site photocatalysts to form well-controlled sized metal particles from the mixture of single-site photocatalysts in the aqueous solution with metal precursors. Under UV-light irradiation of the slurry of TS-1 zeolite in an aqueous $PdCl_2$ solution, the Pd metal can be successfully deposited on the TS-1 (Pd/Ti = 0.6).[49] Similarly, Pt metal was deposited directly from an aqueous solution of H_2PtCl_6 on the photoexcited tetrahedrally coordinated Ti oxide moieties of Ti-HMS mesoporous silica (Pt/Ti = 0.5).[48] These results indicate that the presence of photoexited state of Ti oxide moieties is indispensable for the deposition of metal species. The Fourier transforms of Pd K-edge EXAFS spectra of the Pd/TS-1 catalysts are shown in Figure 9. The presence of the peak assigned to the Pd–Pd bond

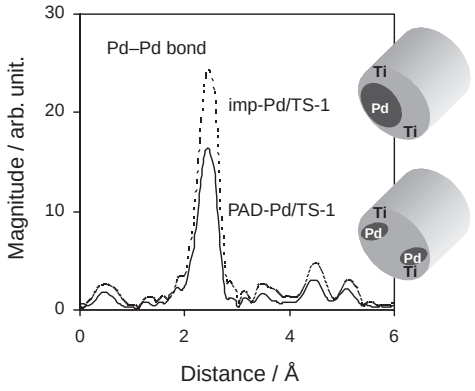

Figure 9. The Fourier transforms of Pd K-edge EXAFS spectra of PAD-Pd/TS-1 (solid line) and imp-Pd/TS-1 (dotted line) after H_2 treatment at 473 K.

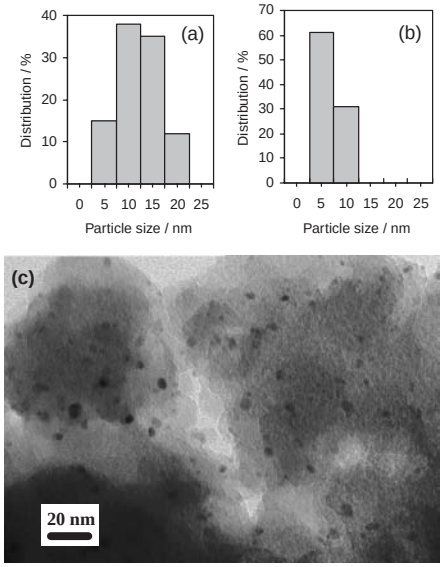

Figure 10. Size distribution diagrams of (a) imp-Pt/Ti-HMS and (b) PAD-Pt/Ti-HMS and (c) TEM image of PAD-Pt/Ti-HMS.

of Pd metal indicates the formation of nano-sized Pd metal. The intensity of the Pd–Pd peak of the photodeposited catalyst (PAD-Pd/TS-1) is smaller than the Pd metal powder and the impregnated catalyst (imp-Pd/TS-1). These results clearly suggest that the smaller Pd metal particles are formed on the photodeposited catalyst (PAD-Pd/TS-1) than the impregnated catalyst (imp-Pd/TS-1). The TEM images show that the PAD-Pt/Ti-HMS has nano-sized Pt metal with well-controlled size of about 4–5 nm as shown in Figure 10, while the imp-Pt/Ti-HMS has Pt metal particles with various sizes in 2–20 nm. Similar phenomena were also observed in the case of the PAD-Pd/TS-1. The highly dispersed deposition of metal precursors on the photoexcited Ti oxide moieties may play an important role for the formation of size-controlled metal particles.

The nano-sized metal catalysts can be applied to the catalytic reactions with high efficiency.[48,49] With the flow of H_2 and O_2 into the aqueous slurry of the Pd/TS-1, H_2O_2 can be produced. As shown in Figure 11, the PAD-Pd/TS-1 can exhibit the higher

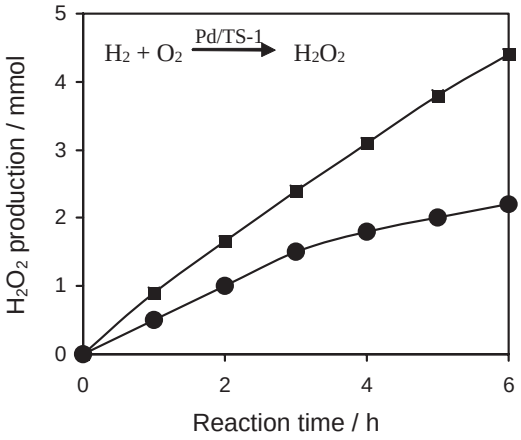

Figure 11. The reaction time profiles of H_2O_2 formation on the PAD-Pd/TS-1 (■) and imp-Pd/TS-1 (●) catalysts in water with a flow of H_2 and O_2. Reaction conditions: Pd/TS-1 (0.1 g), 0.01 M HCl (50 mL), flow of H_2 and O_2 (80 mL·min^{-1}, H_2:O_2 = 1:1) at room temperature.

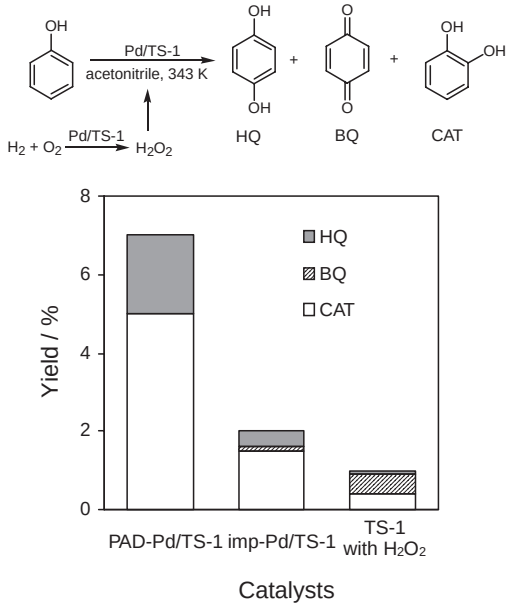

Figure 12. The oxidation of phenol in a flow of H_2 and O_2 on the Pd/TS-1 catalyst. The reaction was carried out in the slurry of catalysts and acetonitrile with 0.01 M HCl in a flow of H_2 and O_2 (80 mL·min^{-1}) for 6 h at 343 K.

reactivity than the imp-Pd/TS-1. The high dispersion of Pd metal particle in the PAD-Pd/TS-1 is preferable for the formation of H_2O_2. Furthermore, using in situ produced H_2O_2 from H_2 and O_2 as an oxidant, the oxidation of phenol can be catalyzed by the tetrahedrally coordinated Ti-oxide moieties of the PAD-Pd/TS-1, as shown in Figure 12. The PAD-Pd/TS-1 exhibited the higher catalytic activity for the oxidation of phenol than the imp-Pd/TS-1 catalyst. The catalytic activity of the PAD-Pd/TS-1 using H_2 and O_2 exceeded that of the TS-1 in the presence of the 30% aq H_2O_2 solution. The micropores and the tetrahedrally coordinated Ti oxide moieties of TS-1 zeolite are suitable for the partial oxidation of phenol with H_2O_2 which are formed

from H_2 and O_2 on the nano-sized Pd metal photodeposited on TS-1. It was also found that the PAD-Pt/Ti-HMS exhibited the higher reactivity than the imp-Pt/HMS for various catalytic reactions such as decomposition of NO diluted in air and CO oxidation.

H. Yamashita and K. Mori appreciate Profs. M. Anpo (Osaka Pref. Univ.), N. Nishiyama (Osaka Univ.), Y. Ichihashi (Kobe Univ.), K. Ikeue (Kumamoto Univ.) for their fruitful discussions and useful advices on this investigation. The present work is supported by the Grant-in-Aid for Scientific Research (KAKENHI) from Ministry of Education, Culture, Sports, Science and Technology. The X-ray adsorption experiments were performed at the SPring-8 and KEK-PF.

References and Notes

1 J. M. Thomas, G. Sankar, *Acc. Chem. Res.* **2001**, *34*, 571.
2 J. M. Thomas, R. Raja, D. W. Lewis, *Angew. Chem., Int. Ed.* **2005**, *44*, 6456.
3 P. Wu, T. Tatsumi, *Catal. Surv. Asia* **2004**, *8*, 2004.
4 A. Corma, *Chem. Rev.* **1997**, *97*, 2373.
5 M. Anpo, M. Che, *Adv. Catal.* **2000**, *44*, 119.
6 M. Anpo, *Bull. Chem. Soc. Jpn.* **2004**, *77*, 1427.
7 H. Yamashita, M. Anpo, *Catal. Surv. Asia* **2004**, *8*, 35.
8 H. Yamashita, M. Anpo, *Curr. Opin. Solid State Mater. Sci.* **2004**, *7*, 471.
9 M. Anpo, J. M. Thomas, *Chem. Commun.* **2006**, 3273.
10 H. Yamashita, M. Matsuoka, K. Tsuji, Y. Shioya, M. Anpo, *J. Phys. Chem.* **1996**, *100*, 397.
11 W.-S. Ju, M. Matsuoka, K. Iino, H. Yamashita, M. Anpo, *J. Phys. Chem. B* **2004**, *108*, 2128.
12 H. Yamashita, Y. Ichihashi, M. Anpo, M. Hashimoto, C. Louis, M. Che, *J. Phys. Chem.* **1996**, *100*, 16041.
13 H. Yamashita, S. G. Zhang, Y. Ichihashi, Y. Matsumura, Y. Souma, T. Tatsumi, M. Anpo, *Appl. Surf. Sci.* **1997**, *121–122*, 305.
14 Y. Ichihashi, H. Yamashita, M. Anpo, Y. Souma, Y. Matsumura, *Catal. Lett.* **1998**, *53*, 107.
15 N. U. Zhanpeisov, M. Matsuoka, H. Mishima, H. Yamashita, M. Anpo, *J. Phys. Chem. B* **1998**, *102*, 6915.
16 J. Zhang, M. Minagawa, T. Ayusawa, S. Natarajan, H. Yamashita, M. Matsuoka, M. Anpo, *J. Phys. Chem.* **2000**, *104*, 11501.
17 M. Anpo, H. Yamashita, Y. Ichihashi, Y. Fujii, M. Honda, *J. Phys. Chem. B* **1997**, *101*, 2632.
18 H. Yamashita, Y. Fuji, Y. Ichihashi, S. G. Zhang, K. Ikeue, D. R. Park, K. Koyano, T. Tatsumi, M. Anpo, *Catal. Today* **1998**, *45*, 221.
19 K. Ikeue, H. Yamashita, T. Takewaki, M. Anpo, *J. Phys. Chem. B* **2001**, *105*, 8350.
20 H. Yamashita, K. Ikeue, T. Takewaki, M. Anpo, *Top. Catal.* **2002**, *18*, 95.
21 H. Yamashita, Y. Ichihashi, M. Harada, G. Stewart, M. A. Fox, M. Anpo, *J. Catal.* **1996**, *158*, 97.
22 H. Yamashita, S. Kawasaki, Y. Ichihashi, M. Harada, M. Anpo, G. Stewart, M. A. Fox, C. Louis, M. Che, *J. Phys. Chem. B* **1998**, *102*, 5870.
23 H. Yamashita, M. Honda, M. Harada, Y. Ichihashi, M. Anpo, Y. Hatano, *J. Phys. Chem. B* **1998**, *102*, 10707.
24 H. Yamashita, H. Nakao, M. Okazaki, M. Anpo, *Stud. Surf. Sci. Catal.* **2003**, *146*, 795.
25 H. Yamashita, K. Maekawa, H. Nakao, M. Anpo, *Appl. Surf. Sci.* **2004**, *237*, 393.
26 H. Yamashita, S. Kawasaki, S. Yuan, K. Maekawa, M. Anpo, M. Matsumura, *Catal. Today*, in press.
27 H. Yamashita, M. Ariyuki, S. Higashimoto, S. G. Zhang, J. S. Chang, S. E. Park, J. M. Lee, Y. Matsumura, M. Anpo, *J. Synchrotron Radiat.* **1999**, *6*, 453.
28 H. Yamashita, K. Yoshizawa, M. Ariyuki, S. Higashimoto, M. Che, M. Anpo, *Chem. Commun.* **2001**, 435.
29 H. Yamashita, K. Yoshizawa, M. Ariyuki, S. Higashimoto, M. Anpo, *Stud. Surf. Sci. Catal.* **2002**, *141*, 495.
30 H. Yamashita, S. Ohshiro, K. Kida, K. Yoshizawa, M. Anpo, *Res. Chem. Intermed.* **2003**, *29*, 881.
31 H. Yamashita, M. Ariyuki, K. Yoshizawa, K. Kida, S. Ohshiro, M. Anpo, *Res. Chem. Intermed.* **2004**, *30*, 235.
32 C. Murata, H. Yoshida, T. Hattori, *Chem. Commun.* **2001**, 2412.
33 Y. Shiraishi, Y. Toshima, T. Hirai, *Chem. Commun.* **2005**, 4569.
34 M. Anpo, S. G. Zhang, S. Higashimoto, M. Matsuoka, H. Yamashita, Y. Ichihashi, Y. Matsumura, Y. Souma, *J. Phys. Chem. B* **1999**, *103*, 9295.
35 S. Higashimoto, M. Matsuoka, H. Yamashita, M. Anpo, O. Kitao, H. Hidaka, M. Che, E. Giamello, *J. Phys. Chem. B* **2000**, *104*, 10288.
36 F. Amano, T. Tanaka, *Chem. Lett.* **2006**, *35*, 468.
37 S. Higashimoto, Y. Hu, R. Tsumura, K. Iino, M. Matsuoka, H. Yamashita, Y. G. Shul, M. Che, M. Anpo, *J. Catal.* **2005**, *235*, 272.
38 N. Ichikuni, T. Eguchi, H. Murayama, K. K. Bando, S. Shimazu, T. Uematsu, *Stud. Surf. Sci. Catal.* **2003**, *146*, 359.
39 H. Yamashita, K. Kida, K. Ikeue, Y. Kanazawa, K. Yoshizawa, M. Anpo, *Stud. Surf. Sci. Catal.* **2003**, *146*, 597.
40 H. Yamashita, Y. Kanazawa, K. Kida, M. Anpo, *Phys. Scr.* **2005**, *T115*, 467.
41 R. Wang, K. Hashimoto, A. Fujishima, M. Chikuni, E. Kojima, A. Kitamura, M. Shimohigoshi, T. Watanabe, *Nature* **1997**, *388*, 431.
42 H. Yamashita, S. Nishio, I. Katayama, N. Nishiyama, H. Fujii, *Catal. Today* **2006**, *111*, 254.
43 K. Mori, S. Imaoka, S. Nishio, Y. Nishiyama, N. Nishiyama, H. Yamashita, *Microporous Mesoporous Mater.*, in press.
44 H. Yamashita, S. Nishio, S. Imaoka, M. Shimada, K. Mori, T. Tanaka, N. Nishiyama, *Top. Catal.*, in press.
45 H. Yamashita, O. Chiyoda, Y. Masui, S. Ohshiro, K. Kida, M. Anpo, *Stud. Surf. Sci. Catal.* **2005**, *158*, 43.
46 Y. Masui, S. Ohshiro, M. Anpo, T. Ohmichi, I. Katayama, H. Yamashita, *e-J. Surf. Sci. Nanotech.* **2005**, *3*, 448.
47 K. Mori, T. Hara, T. Mizugaki, K. Ebitani, K. Kaneda, *J. Am. Chem. Soc.* **2004**, *126*, 10657.
48 H. Yamashita, T. Shimizu, M. Shimada, N. Mimura, K. Mori, M. Sakata, H. Mori, T. Ohmichi, I. Katayama, *Stud. Surf. Sci. Catal.*, in press.
49 H. Yamashita, Y. Miura, K. Mori, T. Ohmichi, T. Sakata, H. Mori, *Catal. Lett.*, in press.